catalysts

MDPI

Article

Pt/C-TiO_2 as Oxygen Reduction Electrocatalysts against Sulfur Poisoning

Yuxin Liu [1,2], Jing Ye [2], Fanpeng Kong [2], Chunyu Du [2], Pengjian Zuo [2], Lei Du [3,*] and Geping Yin [2,*]

[1] College of Chemical and Environmental Engineering, Yancheng Teachers University, Yancheng 224051, China; liuyuxin_hit@126.com
[2] School of Chemistry and Chemical Engineering, Harbin Institute of Technology, 92 West Dazhi St., Harbin 150001, China; ching_yip@foxmail.com (J.Y.); fpkong@hit.edu.cn (F.K.); cydu@hit.edu.cn (C.D.); zuopj@hit.edu.cn (P.Z.)
[3] Huangpu Hydrogen Innovation Center, School of Chemistry and Chemical Engineering, Guangzhou University, Guangzhou 510006, China
* Correspondence: lei.du@gzhu.edu.cn (L.D.); yingeping@hit.edu.cn (G.Y.)

Abstract: Proton exchange membrane (PEM) fuel cells using Pt-based materials as electrocatalysts have achieved a decent performance, represented by the launched Toyota Mirai vehicle. The ideal PEM fuel cells consume stored pure hydrogen and air. However, SO_2, as a primary air contaminant, may be fed along with air at the cathode, leading to Pt site deactivation. Therefore, it is important to improve the SO_2 tolerance of catalysts for the stability of the oxygen reduction reaction (ORR). In this work, we develop the Pt/C-TiO_2 catalyst against SO_2 poisoning during ORR. Impressively, the hybrid Pt/C-TiO_2 catalyst with 20 mass % TiO_2 shows the best ORR and anti-toxic performance: the kinetic current density of ORR is 20.5% higher and the degradation rate after poisoning is 50% lower than Pt/C. The interaction between Pt and TiO_2 as well as the abundant hydroxyl groups on the surface of TiO_2 are both revealed to account for the accelerated removal of poisonous SO_2 on Pt surfaces.

Keywords: electrocatalysis; oxygen reduction reaction; sulfur dioxide; durability

check for updates

Citation: Liu, Y.; Ye, J.; Kong, F.; Du, C.; Zuo, P.; Du, L.; Yin, G. Pt/C-TiO_2 as Oxygen Reduction Electrocatalysts against Sulfur Poisoning. *Catalysts* **2022**, *12*, 571. https://doi.org/10.3390/catal12050571

Academic Editor: Nicolas Alonso-Vante

Received: 19 April 2022
Accepted: 18 May 2022
Published: 23 May 2022

1. Introduction

The PEM fuel cell has been considered as one of the most promising automobile power supplies owing to its high energy efficiency and environmental benefits [1–3]. Delightfully, the first-generation Toyota Mirai has provided an excellent example, using PtCo as a cathode catalyst, achieving a max power with 114 kW and an endurance mileage of up to 502 km. However, the widespread implementation of PEM fuel cells is facing a greatly challenging poisoning/degradation problem caused by impurities such as SO_2 and NO_x in the air, which is ideally supplied directly to the cathodes [4,5]. In particular, SO_2 can strongly adsorb onto the Pt surface and deactivate the active sites for the oxygen reduction reaction (ORR), leading to the degradation of ORR performance [6–13]. For example, it has been reported that the continuous feeding of 2.5 ppm SO_2/air mixture for 45 h at the cathode significantly reduced the fuel cell performance by 53% and, importantly, the subsequent continuous clean air feeding for 20 h could not completely recover the performance [14]. This is because the widely accepted Pt/C catalysts are not efficient enough to remove the S_x species once the coverage is higher than 14%, where up to 95% of mass activity can be lost [15]. In addition, an extremely harsh potential range of 1.2 V~1.5 V is required to completely oxidize SO_x into water-soluble SO_4^{2-} and/or HSO_4^-, which is much higher than the working potential of a PEM fuel cell (0.6 V~0.8 V) [6,16,17]. In this regard, the poisoning SO_2 species is almost irreversible under the normal operating conditions of a PEM fuel cell [18]. This fact triggers us to explore innovations in developing advanced anti-poisoning catalysts.

Numerous efforts have been made to prevent Pt-based catalysts from SO_2 poisoning [19]. For example, Baturina and coworkers [20,21] found that the adsorbed SO_2 is more easily oxidized and removed on Pt_3Co/C than Pt/C, although the alloying Pt_3Co/C catalyst is more sensitive to the poisoning (The same concentration of SO_2 has a more serious effect on the ORR performance of Pt_3Co/C). They found that H_2O is more likely to decompose into hydroxyl (-OH) on Pt_3Co/C, which is beneficial for accelerating the electro-oxidation of SO_2. In addition, Xu et al. [22] found that the SO_2-poisoned 5 mass % WO_x–Pt/C can cause a higher loss of SO_2 than commercial Pt/C after the first potential cycling up to 1.5 V, which might be due to the synergistic effect between WO_x and Pt. The OH group on the hydrophilic WO_x surface and the hydrogen spillover effect promote the electro-oxidation of sulfur-containing species. In their latter work, the $Pt/CeO_2/C$ catalyst was prepared by one-pot synthesis, enhancing the oxygen migration and thus improving SO_2 electro-oxidation and ORR activity [23,24]. In our previous work, we found that Ru efficiently modified the electronic structure of Pt in PtRu alloy catalysts, leading to a weaker interaction between Pt and SO_2 [25]. In this work, we will focus on the effect of metal oxides to the ORR performance and SO_2 tolerance of Pt.

To tone-up the positive effects of oxidative hydroxyl and synergy, we herein develop a hybrid Pt/C-TiO_2 catalyst against SO_2 poisoning during ORR. The selection of TiO_2 is based on its high hydrophilicity and outstanding chemical and electrochemical stability, as well as strong interaction with the Pt component [26–33]. Importantly, based on the above discussions, the abundant hydroxyl groups (-OH) on the hydrophilic TiO_2 surface may benefit poisonous sulfur removal. Accordingly, the electro-oxidation of SO_2 is significantly accelerated on such a Pt/C-TiO_2 catalyst to reduce the SO_2 poisoning. To our knowledge, the effect of TiO_2 on suppressing SO_2 poisoning of Pt-based ORR catalysts has not been reported. In this work, our hybrid Pt/C-TiO_2 catalysts have higher ORR activity and better sulfur tolerance compared to traditional Pt/C.

2. Results and Discussion

2.1. Characterization of Catalysts

Figure 1 shows the X-ray diffraction (XRD) patterns of the as-prepared Pt/C, Pt/C-20TiO_2 catalysts and TiO_2 nanoparticles. For the Pt/C sample, the broad X-ray diffraction peak in the range of 20°~30° corresponds to the amorphous structure of XC-72 carbon black, while the peaks at 39.8°, 46.2°, 67.5°, and 81.3° correspond to Pt(111), (200), (220), and (311) facets, respectively (JCPDS No. 04-0802). The commercial TiO_2 sample shows sharp peaks, which can be indexed to the anatase TiO_2 (JCPDS No. 21-1272). The XRD pattern of Pt/C-20TiO_2 has the X-ray diffraction peaks of both Pt and TiO_2. The above facts demonstrate that the Pt/C and Pt/C-20TiO_2 were synthesized successfully.

As the high-resolution transmission electron microscopy (HRTEM) image in Figure 2a shows, the Pt nanoparticles are uniformly dispersed on the carbon supports with an average size of about 2.74 nm (Figure S1). A small Pt particle size and uniform dispersion potentially ensure good catalytic performance [34]. Figure 2b shows TEM images of the as-prepared Pt/C-20TiO_2 catalyst. The lattice fringes of 0.35 nm (red tags) and 0.22 nm (yellow tags) are assigned to the TiO_2 (101) plane and the Pt (111) plane, respectively. It can be seen that the TiO_2 and Pt particles are well contacted with each other.

2.2. Electrocatalytic Performance

The cyclic voltammogram (CV) and linear sweep voltammetry (LSV) curves of all pristine catalysts (before poisoning) are shown in Figure 3a,b, respectively. The electrochemical surface areas (ECSAs) of all the catalysts were calculated based on the H_2 adsorption/desorption region at 0~0.3 V in CV curves. All the relevant data recorded and calculated from electrochemical measurement are listed in Table 1.

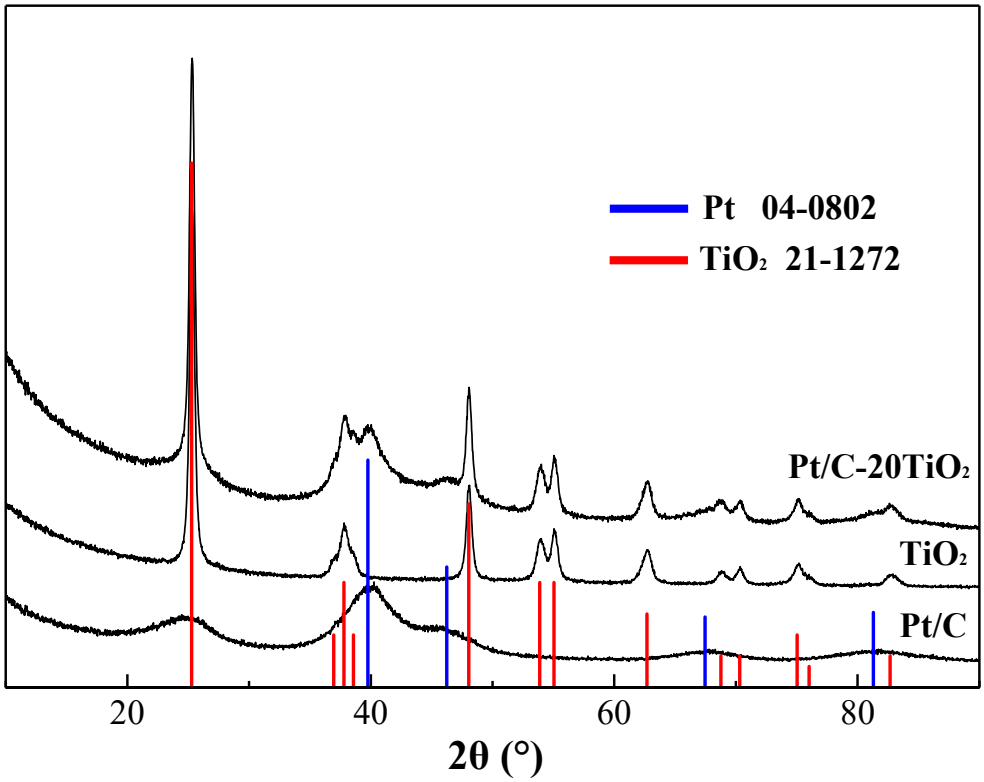

Figure 1. XRD patterns of Pt/C, commercial TiO_2 and Pt/C-20TiO_2 catalysts.

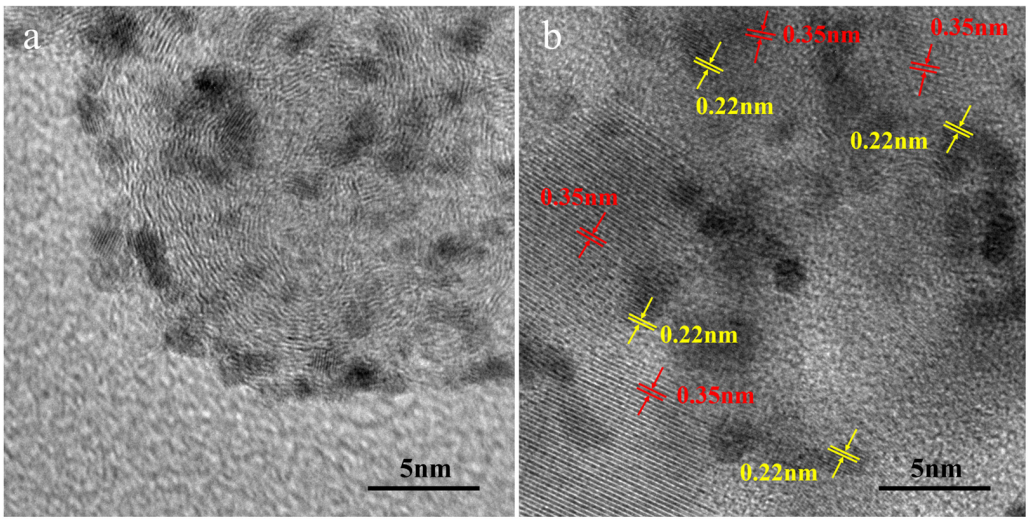

Figure 2. (**a**) TEM images of Pt/C and (**b**) Pt/C-20TiO_2 catalysts.

The results show that the addition of TiO_2 has little effect on the ECSA of the Pt/C catalyst. Compared with that of Pt/C, the current peak, representing the oxygen reduction of the Pt/C-TiO_2 catalysts, shifts positively when $TiO_2 \leq 30\%$; Pt/C-20TiO_2 has the most positive oxygen reduction peak, which likely indicates the best ORR activity, consistent with the LSV results in Figure 3b. The activity towards ORR is improved by increasing TiO_2 content and then started to decrease after reaching a maximum value, i.e., Pt/C-20TiO_2. Too much TiO_2 ($\geq$30 mass %) hinders the ORR activity, which is due to the low electron conductivity of TiO_2. On the other hand, the half-wave potential ($E_{1/2}$) of Pt/C-20TiO_2 is 0.867 V, presenting an increase by 0.014 V compared with Pt/C (0.853 V), and the i_k @ 0.9 V is 2.337 mA/cm^2, 20.5% higher than Pt/C (1.939 mA/cm^2). Based on the Koutechy–Levich (K–L) equation (see Section 3.3), the ORR polarization curves of Pt/C-20TiO_2 were

measured at different rotation speeds (Figure S2a). The charge transfer electrons (n) of Pt/C-20TiO_2 can be derived from the slopes of the liner K-L plot (Figure S2b), which are 3.89, 3.87, 3.87, and 3.86 at 0.75 V, 0.7 V, 0.65 V, and 0.6 V, respectively, indicating the four-electron reaction pathway of ORR. This fact demonstrates the positive effect of TiO_2 for ORR activity.

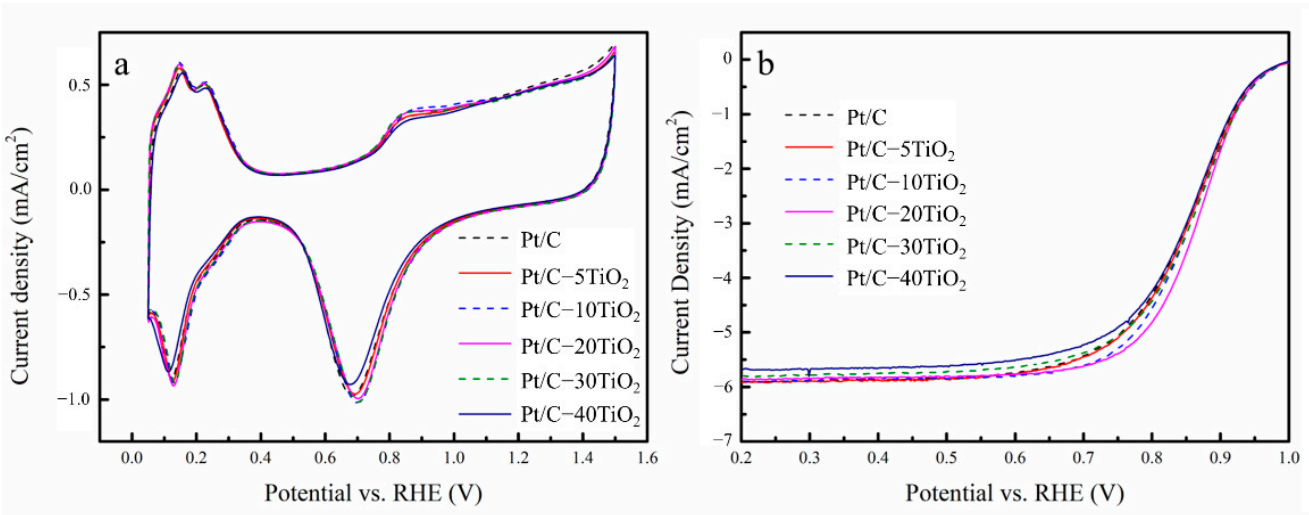

Figure 3. The (**a**) CV and (**b**) LSV curves of all pristine catalysts (before poisoning).

Table 1. Electrochemical data of all pristine (before poisoning) and SO_2-poisoned catalysts.

Sample	Pristine			SO_2 Poisoned			Negative Shift of $E_{1/2}$ after Poisoning (mV)	Loss of i_k @ 0.9 V after Poisoning
	ECSA (m^2 g_{Pt}^{-1})	$E_{1/2}$ (V)	i_k@ 0.9 V (mA cm^{-2})	ECSA (m^2 g_{Pt}^{-1})	$E_{1/2}$ (V)	i_k@ 0.9 V (mA cm^{-2})		
Pt/C	97.07	0.853	1.939	27.06	0.782	0.624	71	67.8%
Pt/C-5TiO_2	97.84	0.855	2.042	26.55	0.800	1.175	55	42.5%
Pt/C-10TiO_2	102.04	0.858	2.172	28.32	0.809	1.424	49	34.4%
Pt/C-20TiO_2	101.46	0.867	2.337	25.99	0.814	1.517	53	35.1%
Pt/C-30TiO_2	99.11	0.86	2.210	29.82	0.775	0.801	85	63.7%
Pt/C-40TiO_2	95.11	0.855	1.884	26.81	0.736	0.716	119	62.0%

The first CV scans of each catalyst after poisoning in Ar-saturated 0.1 M $HClO_4$ solution are shown in Figure 4a, where the ECSA of all the catalysts decreases in a similar way because the strongly adsorbed SO_2 blocks the active site of Pt. In addition, clear oxidation peaks are observed in the potential range of 0.8 V~1.5 V, due to the electrochemical oxidation of SO_2. Notably, there is a negative shift in the SO_2 oxidation peak of Pt/C-TiO_2 catalysts compared with Pt/C, indicating the higher activity of Pt/C-TiO_2 catalysts to oxidize SO_2. Particularly, the Pt/C-20TiO_2 has the largest negative shift by about 50 mV in SO_2 oxidation, as shown in Figure 4b. The oxide reduction potential region of Figure 4b is magnified and shown in Figure 4c to compare the catalytic performance of Pt/C and Pt/C-20TiO_2 before and after poisoning. It is clear that the reduction peaks of Pt/C-20TiO_2 before or after poisoning all positively shift compared with the Pt/C catalyst, indicating that the Pt/C-20TiO_2 has a better electrocatalytic performance to reduce oxygen-bearing species than Pt/C at initial and after sulfur poisoning.

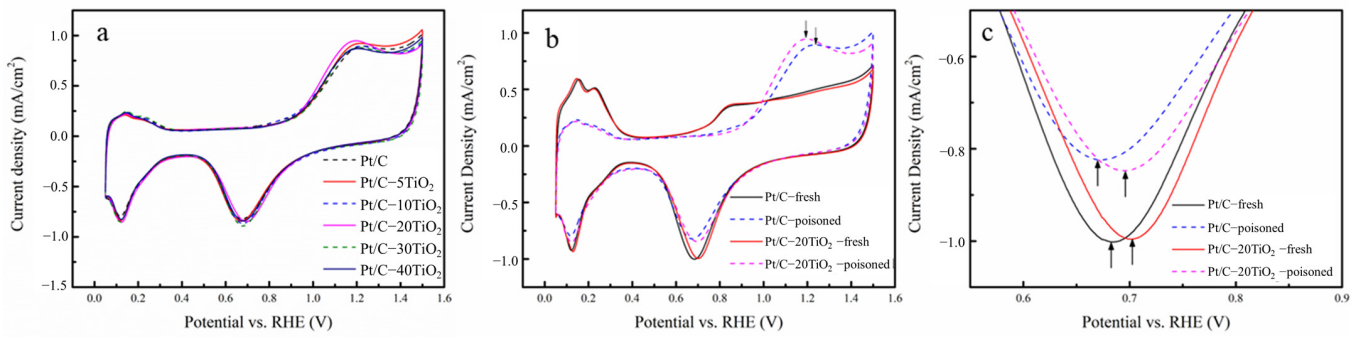

Figure 4. CV curves in Ar-saturated 0.1 M $HClO_4$ solution of (**a**) all catalysts after SO_2 poisoning, (**b**) Pt/C and Pt/C−20TiO_2 before and after poisoning, and (**c**) corresponding magnification at oxide reduction potential region.

The LSV curves of ORR after SO_2 poisoning are shown in Figure 5a. After SO_2 poisoning, the ORR activity of all catalysts is decreased, although the Pt/C-20TiO_2 catalyst still has the best ORR activity. The i_k@ 0.9 V comparison between the fresh and poisoned catalysts is shown in Figure 5b. With the addition of TiO_2, the decrease percentage of kinetic current density is significantly lowered. The Pt/C-10TiO_2 and Pt/C-20TiO_2 catalysts have the smallest activity decay by only 34.4% and 35.1%, respectively, in contrast to 67.8% for Pt/C. Table 1 shows that the $E_{1/2}$ of Pt/C-20TiO_2 went down by 53 mV negatively after poisoned, much lower than the 71 mV of Pt/C. All this indicates that the SO_2 tolerance of Pt/C-20TiO_2 is greatly improved than Pt/C.

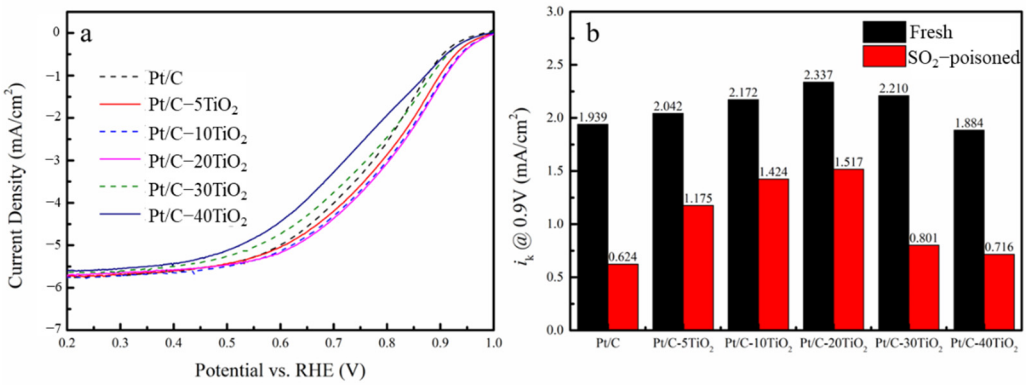

Figure 5. (**a**) The LSV ORR curves of SO_2 poisoned catalysts; (**b**) the kinetic current density at 0.9 V of fresh and SO_2−poisoned catalysts.

2.3. Mechanism of SO_2 Tolerance

The X-ray photoelectron spectroscopy (XPS) spectra of the O 1s, Ti 2p and Pt 4f regions in TiO_2, Pt/C, and Pt/C-20TiO_2 are shown in Figure 6. As shown in the O 1s region (Figure 6a), the peaks at 533.5 ± 0.1 eV, 532.2 ± 0.1 eV and 530.6 ± 0.1 eV are assigned to physically absorbed water (O1), chemisorbed OH species (O2), and lattice oxygen in TiO_2 and/or PtO (O3) [26,35]. In addition, it can be seen that the Ti 2p binding energy of Pt/C-20TiO_2 has a negative shift by 0.4 eV compared with Pt/C (Figure 6b). The Pt 4f regions for Pt/C and Pt/C-20TiO_2 can be fitted into three sets of doublets (Figure 6c). For the Pt/C, Pt 4f peaks at 71.4 eV and 74.7 eV are assigned to Pt (0), 72.8 eV and 76.1 eV to Pt (II) in PtO or $Pt(OH)_2$-like species, and 74.0 eV and 77.3 eV to Pt(IV) in PtO_2. Interestingly, the binding energy of the Pt/C-20TiO_2 catalyst is negatively shifted by 0.3 eV compared to the Pt/C catalyst, indicating an electronic interaction between Pt and TiO_2.

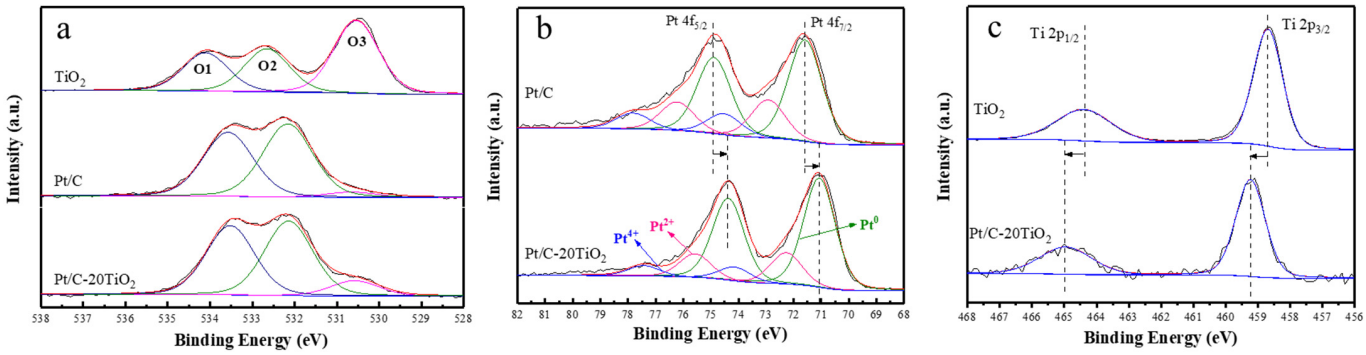

Figure 6. XPS spectra in (**a**) O 1s region of TiO_2, Pt/C and Pt/C−20TiO_2; (**b**) Ti 2p XPS of TiO_2 and Pt/C−20TiO_2; (**c**) Pt 4f XPS of Pt/C and Pt/C−20TiO_2.

The electron transfer from TiO_2 to Pt increases the electron density of Pt, which was reported as a necessity for effective ORR [36]. In addition, the binding energy between Pt and OH-like oxygen-containing species is weakened, which accelerates the reaction of O, OH, and H^+ to generate H_2O and improves the ORR activity [37,38]. Jaksic et al. [39] found that in aqueous media, OH on the surface of metal oxides such as WO_3 and TiO_2 can be transferred to the Pt surface to form Pt-OH, which is the so-called spillover effect. Reasonably, such an OH spillover effect of TiO_2 will repel the OH groups on Pt, leading to decreased binding energy between OH and Pt and promoting ORR activity [40]. On the other hand, the electronic interaction between Pt and TiO_2 is able to weaken the adsorption of poisoning species on Pt surfaces [25,41]. At the same time, the spillover effect of oxidative OH on the TiO_2 surface plays a significant role in promoting the electro-oxidation (removal) of SO_2 [22]. Figure 7 is provided to illustrate this mechanism. For the Pt/C-TiO_2 catalyst: Pt provides electrocatalytic active sites for oxygen reduction; C supports Pt nanoparticles and conducts electrons; and TiO_2 modifies the electronic structure of Pt to enhance the ORR activity and SO_2 tolerance.

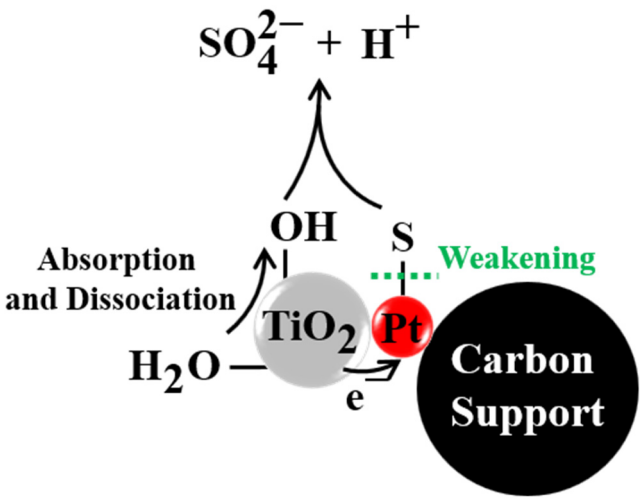

Figure 7. The schematic diagram of SO_2 electro-oxidation mechanism on Pt/C−TiO_2 catalysts.

3. Materials and Methods

3.1. Chemicals and Materials Characterization

Chloroplatinic acid (H_2PtCl_6, Sinopharm Chemical Reagent), Vulcan carbon XC-72 (Cabot Corp, Boston, MA, USA), TiO_2 nanoparticles (25 nm, anatase, Aladdin, Shanghai, China), perchloric acid ($HClO_4$, Aladdin, Shanghai, China), anhydrous sodium sulfite (Na_2SO_3, Dupont, Eleutherian Mills, DE, USA), and 5.0 wt % Nafion aqueous solution (Dupont, Eleutherian Mills, DE, USA) were of analytical grade and used as received if not

specified. Deionized water (18.2 MΩ cm, Mill-Q Corp, Darmstadt, Germany) was used in all of the experiments.

TEM and HRTEM images were taken on JEOL JEM-2100 with an acceleration voltage of 300 kV. The morphologies and crystal structure of the Pt/C, Pt/C-TiO_2 catalyst and TiO_2 nanoparticles were characterized by XRD (Netherlands, Panalytical X'PERT) using Cu Kα radiation. XPS measurements were performed by a Physical Electronics PHI model 5700 instrument with an electron energy analyzer, with half-spherical precision using Al Kα radiation (1486.6 eV). The binding energy of all samples was calibrated vs. the C 1s value of 284.6 eV.

3.2. Synthesis of Catalysts

The Pt/C catalyst (20 mass % Pt) was prepared by the microwave-assisted polyol reduction method [42]. Briefly, 40 mg Vulcan XC-72 carbon black was well-dispersed into 60 mL ethylene glycol (EG) and isopropanol (*V*/*V* = 4:1) under ultrasonic treatment for 2 h. Then H_2PtCl_6-EG solution was added to the slurry and stirred constantly for 2 h. Next, 1 mol/L NaOH-EG solution was dropped into the slurry under continuous stirring until the pH was stable at 12. Argon was injected into the slurry for 20 min to remove oxygen, which was then placed in a microwave oven (2450 MHz, 800 W) and heated for 2 min. After the solution was cooled down to room temperature, a certain amount of dilute nitric acid was added to pH = 3, followed by stirring for 12 h. After washing with plenty of boiling ultra-pure water (Milli-Q, 18 MΩ cm), the Pt/C catalyst was dried in a vacuum oven at 70 °C for 12 h.

The Pt/C catalyst ink was prepared by dispersing 5 mg Pt/C catalyst into a mixture of 5 μL of 5 wt.% Nafion solution, 1.25 mL isopropanol, and 3.75 mL ultra-pure water. For the hybrid Pt/C-TiO_2 catalyst ink, a certain amount of TiO_2 nanoparticles were first dispersed in 3.75 mL ultra-pure water, prior to adding and dispersing 5 mg Pt/C, 5 μL Nafion solution, and 1.25 mL isopropanol. The hybrid catalysts were labeled as Pt/C-5TiO_2, Pt/C-10TiO_2, Pt/C-20TiO_2, Pt/C-30TiO_2, and Pt/C-40TiO_2 using different TiO_2 contents of 5, 10, 20, 30, and 40 mass %.

3.3. Electrochemical Measurements

All electrochemical measurements were carried out in a three-electrode system with an electrolyte of 0.1 mol/L $HClO_4$ aqueous solution at room temperature, using the glassy carbon rotating-disk electrode (GC-RDE, 5 mm in diameter) as the working electrode, a saturated Ag-AgCl electrode as the reference electrode, and a piece of Pt foil (1 cm^2) as the counter electrode. 10 μL of catalyst ink was dropped onto the polished GC-RDE. Then the electrodes were air-dried at room temperature. The catalyst loading was about 10 μg/cm^2.

The ECSA of the catalyst is calculated based on the charge number of H adsorption or desorption, as shown in Equation (1).

$$\mathrm{ECSA} = \frac{Q_{\mathrm{H}}}{0.21 \times 10^{-3} \times m_{\mathrm{Pt}}} \tag{1}$$

where Q_{H} (C) represents the charge number of H adsorption or desorption and can be obtained by integrating the CV curve in Ar-saturated 0.1 mol L^{-1} $HClO_4$ solution between 0.05 and 0.4 V; and m_{Pt} (g) is the Pt load in the catalyst. Assuming there is a one-to-one relationship between the Pt atom and H atom of the hydrogen monatomic layer on the Pt/C catalyst, the charge amount of the hydrogen monatomic layer on the Pt/C catalyst surface is 210 μC cm^{-2}.

Before recording ORR activity, ultra-pure argon gas was injected into the electrolyte for 20 min to remove dissolved oxygen. CV scans were then performed at the scan rate of 50 mV s^{-1} in a potential range of 0.05 V~1.5 V for 10 cycles at room temperature. The ORR activity of the catalyst was then measured by LSV from 0.05 V to 1 V at a scan rate of 10 mV s^{-1} at 1600 rpm in O_2-saturated 0.1 mol/L $HClO_4$ solution. The kinetic current

density at 0.9 V and transferred electron number were calculated from the ORR polarization following the Koutechy–Levich (K–L) equation, Equation (2).

$$\frac{1}{i} = \frac{1}{i_k} + \frac{1}{i_d} = \frac{1}{i_k} + \frac{1}{0.62nFAD^{2/3}\omega^{1/2}\nu^{-1/6}c} \quad (2)$$

where i_k and i_d are the kinetic current density and limited diffusion current density, n is the number of electrons transferred, F is the Faraday constant (96,487 C mol^{-1}), A is the geometric surface area of the RDE, c is the bulk concentration of O_2 (2.64×10^{-4} mol cm^{-3}), D is the diffusion coefficient of O_2 (1.93×10^{-5} cm^2 S^{-1}), ν is the kinematic viscosity of the solution (0.01 cm^2 S^{-1}), and ω is the angular velocity. The half-wave potential ($E_{1/2}$) is read from the ORR curve of the catalyst, which is the potential corresponding to the half of the limited diffusion current density.

The poisoning of catalysts was carried out by immerging the working electrode at the potential of 0.65 V for 1 min in a 0.5 mmol/L Na_2SO_3 + 0.1 mol/L $HClO_4$ electrolyte. Then, the GC-RDE was rinsed with ultra-pure water and transferred to a fresh 0.1 mol/L $HClO_4$ electrolyte without SO_2. The ORR activity of the poisoned electrode was evaluated in an O_2-saturated 0.1 mol/L $HClO_4$ electrolyte using LSV at 1600 rpm. To investigate the oxidation behavior of adsorbed SO_2, a CV scan was performed between 0.05 V and 1.5 V for 10 cycles at a sweep rate of 50 mV/s. All of the potentials were reported with respect to the reversible hydrogen electrode (RHE) in this work.

4. Conclusions

Hybrid Pt/C-TiO_2 catalysts were prepared by mixing Pt/C catalyst and TiO_2 nanoparticles. By adding TiO_2, the ORR performances of fresh and SO_2-poisoned catalysts were all improved compared to the Pt/C and the activity loss caused by SO_2 poisoning was remarkably reduced. Our detailed observations indicate that the improved SO_2 tolerance is due to the accelerated electro-oxidation of SO_2 in the presence of optimal TiO_2. We suggest that the electronic interaction between Pt and TiO_2 and the OH spillover effect on TiO_2 might be crucial for not only enhancing the ORR activity, but also removing the poisoning SO_2. These results indicate that the TiO_2 modified Pt/C catalyst is a desired ORR catalyst against sulfur poisoners in PEM fuel cells.

Supplementary Materials: The following supporting information can be downloaded at: https://www.mdpi.com/article/10.3390/catal12050571/s1, Figure S1: TEM images of Pt/C and particle size distributions; Figure S2: The ORR polarization curves of Pt/C-20TiO_2 measured at different electrode rotation speeds and the K-L plots from the polarization curve.

Author Contributions: Synthesis and characterization, Y.L. and J.Y.; electrocatalytic experiments, Y.L. and F.K.; supervision, L.D. and C.D.; project administration, G.Y. and P.Z.; writing, Y.L. and L.D.; proofread, G.Y. and L.D. All authors have read and agreed to the published version of the manuscript.

Funding: This research was funded by the National Key Research and Development Program of China (Program No.2016YFB0101207), Natural Science Research Project of Jiangsu Higher Education Institutions (Grant No.20KJA530004, 21KJA530004), Excellent scientific research and innovation team project of Yancheng Teachers University, and the Outstanding Youth Project of Guangdong Provincial Natural Science Foundation (Grant No. 2022B1515020020).

Data Availability Statement: Data are available in the main text.

Acknowledgments: We acknowledge the financial support from National Key Research and Development Program of China (Program No.2016YFB0101207), Natural Science Research Project of Jiangsu Higher Education Institutions (Grant No.20KJA530004, 21KJA530004), Excellent scientific research and innovation team project of Yancheng Teachers University, and the Outstanding Youth Project of Guangdong Provincial Natural Science Foundation (Grant Number: 2022B1515020020).

Conflicts of Interest: The authors declare no conflict of interest.

References

1. Du, L.; Prabhakaran, V.; Xie, X.; Park, S.; Wang, Y.; Shao, Y. Low-PGM and PGM-free catalysts for proton exchange membrane fuel cells: Stability challenges and material solutions. *Adv. Mater.* **2021**, *33*, 1908232. [CrossRef] [PubMed]
2. Li, H.; Sun, B.; Hao, J.; Zhao, J.; Li, J.; Khakichi, A. Economical planning of fuel cell vehicle-to-grid integrated green buildings with a new hybrid optimization algorithm. *Int. J. Hydrogen Energy* **2022**, *47*, 8514–8531. [CrossRef]
3. Yu, H.; Zhou, T.; Wang, Z.; Xu, Y.; Li, X.; Wang, L.; Wang, H. Defect-Rich Porous Pd Metallene for Enhanced Alkaline Oxygen Reduction Electrocatalysis. *Angew. Chem. Int. Ed. Engl.* **2021**, *133*, 12134–12138. [CrossRef]
4. Singh, P.; Gangadharan, P.K.; Khan, Z.; Kurungot, S.; Jaiswal, A. Cubic palladium nanorattles with solid octahedron gold core for catalysis and alkaline membrane fuel cell Applications. *ChemCatChem* **2019**, *11*, 4383–4392. [CrossRef]
5. Malko, D.; Lopes, T.; Symianakis, E.; Kucernak, A. The intriguing poison tolerance of non-precious metal oxygen reduction reaction (ORR) catalysts. *J. Mater. Chem.* **2016**, *4*, 142–152. [CrossRef]
6. Jing, F.; Hou, M.; Shi, W.; Fu, J.; Yu, H.; Ming, P.; Yi, B. The effect of ambient contamination on PEMFC performance. *J. Power Sources* **2007**, *166*, 172–176. [CrossRef]
7. Garsany, Y.; Gould, B.D.; Baturina, O.A.; Swider-Lyons, K.E. Comparison of the Sulfur Poisoning of PBI and Nafion PEMFC Cathodes. *Electrochem. Solid-State Lett.* **2009**, *12*, B138. [CrossRef]
8. Baturina, O.A.; Gould, B.D.; Korovina, A.; Garsany, Y.; Stroman, R.; Northrup, P.A. Products of SO_2 adsorption on fuel cell electrocatalysts by combination of sulfur K-edge XANES and electrochemistry. *Langmuir* **2011**, *27*, 14930–14939. [CrossRef]
9. Liu, Y.-X.; Zhang, W.-Y.; Han, G.-K.; Zhou, Y.-W.; Li, L.-F.; Kang, C.; Kong, F.-P.; Gao, Y.-Z.; Du, C.-Y.; Wang, J.-J. Deactivation and regeneration of a benchmark Pt/C catalyst toward oxygen reduction reaction in the presence of poisonous SO_2 and NO. *Catal. Sci. Technol.* **2022**, accepted. [CrossRef]
10. Awad, M.I.; Saleh, M.M.; Ohsaka, T. Impact of SO_2 poisoning of platinum nanoparticles modified glassy carbon electrode on oxygen reduction. *J. Power Sources* **2011**, *196*, 3722–3728. [CrossRef]
11. Reshetenko, T.; Laue, V.; Krewer, U.; Artyushkova, K. Study of degradation and spatial performance of low Pt-loaded proton exchange membrane fuel cells under exposure to sulfur dioxide in an oxidant stream. *J. Power Sources* **2020**, *458*, 228032. [CrossRef]
12. Awad, M.I.; Saleh, M.M.; Ohsaka, T. Electroactivity regeneration of sulfur-poisoned platinum nanoparticle-modified glassy carbon electrode at low anodic potentials. *J. Solid State Electrochem.* **2015**, *19*, 1331–1340. [CrossRef]
13. Borup, R.; Weber, A. Fuel Cell Performance and Durability Consortium. Available online: https://www.hydrogen.energy.gov/pdfs/review19/fc135_borup_2019_o.pdf (accessed on 30 April 2019).
14. Mohtadi, R.; Lee, W.K.; Van Zee, J.W. Assessing durability of cathodes exposed to common air impurities. *J. Power Sources* **2004**, *138*, 216–225. [CrossRef]
15. Garsany, Y.; Baturina, O.A.; Swider-Lyons, K.E. Impact of sulfur dioxide on the oxygen reduction reaction at Pt/Vulcan carbon electrocatalysts. *J. Electrochem. Soc.* **2007**, *154*, B670–B675. [CrossRef]
16. Xie, F.; Shao, Z.-G.; Zhang, G.; Zhai, J.; Lu, W.; Qin, X.; Lin, W.; Yi, B. A quantitative research on S- and SO_2-poisoning Pt/Vulcan carbon fuel cell catalyst. *Electrochim. Acta* **2012**, *67*, 50–54. [CrossRef]
17. Liu, Y.X.; Zhang, W.Y.; Han, G.K.; Zhou, Y.W.; Li, L.F.; Kong, F.P.; Gao, Y.Z.; Du, C.Y.; Wang, J.J.; Du, L.; et al. Deactivated Pt Electrocatalysts for the Oxygen Reduction Reaction: The Regeneration Mechanism and a Regenerative Protocol. *ACS Catal.* **2021**, *11*, 9293–9299. [CrossRef]
18. Punyawudho, K.; Ma, S.; Van Zee, J.W.; Monnier, J.R. Effect of O_2 on the adsorption of SO_2 on carbon-supported Pt electrocatalysts. *Langmuir* **2011**, *27*, 7524–7530. [CrossRef]
19. Von Deak, D.; Singh, D.; Biddinger, E.J.; King, J.C.; Bayram, B.; Miller, J.T.; Ozkan, U.S. Investigation of sulfur poisoning of CNx oxygen reduction catalysts for PEM fuel cells. *J. Catal.* **2012**, *285*, 145–151. [CrossRef]
20. Baturina, O.A.; Gould, B.D.; Garsany, Y.; Swider-Lyons, K.E. Insights on the SO_2 poisoning of Pt_3Co/VC and Pt/VC fuel cell catalysts. *Electrochim. Acta* **2010**, *55*, 6676–6686. [CrossRef]
21. Ramaker, D.E.; Gatewood, D.; Korovina, A.; Garsany, Y.; Swider-Lyons, K.E. Resolving Sulfur Oxidation and Removal from Pt and Pt_3Co Electrocatalysts Using in Situ X-ray Absorption Spectroscopy. *J. Phys. Chem. C* **2010**, *114*, 11886–11897. [CrossRef]
22. Xu, R.; Xu, F.; Pan, M.; Mu, S. Improving sulfur tolerance of noble metal catalysts by tungsten oxide-induced effects. *RSC Adv.* **2013**, *3*, 764–773. [CrossRef]
23. Xu, F.; Cheng, K.; Yu, Y.; Mu, S. One-pot synthesis of Pt/CeO_2/C catalyst for enhancing the SO_2 electrooxidation. *Electrochim. Acta* **2017**, *229*, 253–260. [CrossRef]
24. Xu, F.; Wang, D.; Sa, B.; Yu, Y.; Mu, S. One-pot synthesis of Pt/CeO_2/C catalyst for improving the ORR activity and durability of PEMFC. *Int. J. Hydrogen Energy* **2017**, *42*, 13011–13019. [CrossRef]
25. Liu, Y.; Du, L.; Kong, F.; Han, G.; Gao, Y.; Du, C.; Zuo, P.; Yin, G. Sulfur Dioxide-Tolerant Bimetallic PtRu Catalyst toward Oxygen Electroreduction. *ACS Sustain. Chem. Eng.* **2019**, *8*, 1295–1301. [CrossRef]
26. Wang, Y.; Wang, J.; Han, G.; Du, C.; Sun, Y.; Du, L.; An, M.; Yin, G.; Gao, Y.; Song, Y. Superior catalytic performance and CO tolerance of Ru@Pt/C-TiO_2 electrocatalyst toward methanol oxidation reaction. *Appl. Surf. Sci.* **2019**, *473*, 943–950. [CrossRef]
27. Li, Y.; Liu, C.; Liu, Y.; Feng, B.; Li, L.; Pan, H.; Kellogg, W.; Higgins, D.; Wu, G. Sn-doped TiO_2 modified carbon to support Pt anode catalysts for direct methanol fuel cells. *J. Power Sources* **2015**, *286*, 354–361. [CrossRef]
28. Ruiz-Camacho, B.; Martínez-González, J.; González-Huerta, R.; Tufiño-Velazquez, M. Kinetic study of oxygen reduction reaction and PEM fuel cell performance of Pt/TiO_2-C electrocatalyst. *Int. J. Hydrogen Energy* **2014**, *39*, 16731–16739. [CrossRef]

29. Yu, L.; Xi, J. TiO_2 nanoparticles promoted Pt/C catalyst for ethanol electro-oxidation. *Electrochim. Acta* **2012**, *67*, 166–171. [CrossRef]
30. Jiang, Z.-Z.; Wang, Z.-B.; Chu, Y.-Y.; Gu, D.-M.; Yin, G.-P. Ultrahigh stable carbon riveted Pt/TiO_2–C catalyst prepared by in situ carbonized glucose for proton exchange membrane fuel cell. *Energ. Environ. Sci.* **2011**, *4*, 728–735. [CrossRef]
31. Li, B.; Ding, Y.; Li, Q.; Guan, Z.; Zhang, M.; Yang, J. The photothermal effect enhance visible light-driven hydrogen evolution using urchin-like hollow RuO_2/TiO_2/Pt/C nanomaterial. *J. Alloys Compd.* **2022**, *890*, 161722. [CrossRef]
32. Haidry, A.A.; Fatima, Q.; Mehmood, A.; Shahzad, A.; Ji, Y.; Saruhan, B. Adsorption Kinetics of NO_2 Gas on Pt/Cr-TiO_2/Pt-Based Sensors. *Chemosensors* **2021**, *10*, 11. [CrossRef]
33. Vikrant, K.; Weon, S.; Kim, K.-H.; Sillanpää, M. Platinized titanium dioxide (Pt/TiO_2) as a multi-functional catalyst for thermocatalysis, photocatalysis, and photothermal catalysis for removing air pollutants. *Appl. Mater. Today* **2021**, *23*, 100993. [CrossRef]
34. Du, L.; Shao, Y.; Sun, J.; Yin, G.; Liu, J.; Wang, Y. Advanced catalyst supports for PEM fuel cell cathodes. *Nano Energy* **2016**, *29*, 314–322. [CrossRef]
35. Selvarani, G.; Maheswari, S.; Sridhar, P.; Pitchumani, S.; Shukla, A. Carbon-supported Pt–TiO_2 as a methanol-tolerant oxygen-reduction catalyst for DMFCs. *J. Electrochem. Soc.* **2009**, *156*, B1354. [CrossRef]
36. Lewera, A.; Timperman, L.; Roguska, A.; Alonso-Vante, N. Metal–support interactions between nanosized Pt and metal oxides (WO_3 and TiO_2) studied using X-ray photoelectron spectroscopy. *J. Phys. Chem. C* **2011**, *115*, 20153–20159. [CrossRef]
37. Timperman, L.; Lewera, A.; Vogel, W.; Alonso-Vante, N. Nanostructured platinum becomes alloyed at oxide-composite substrate. *Electrochem. Commun.* **2010**, *12*, 1772–1775. [CrossRef]
38. Camacho, B.R.; Morais, C.; Valenzuela, M.; Alonso-Vante, N. Enhancing oxygen reduction reaction activity and stability of platinum via oxide-carbon composites. *Catal. Today* **2013**, *202*, 36–43. [CrossRef]
39. Jaksic, J.M.; Krstajic, N.V.; Vracar, L.M.; Neophytides, S.G.; Labou, D.; Falaras, P.; Jaksic, M.M. Spillover of primary oxides as a dynamic catalytic effect of interactive hypo-d-oxide supports. *Electrochim. Acta* **2007**, *53*, 349–361. [CrossRef]
40. Jaksic, J.M.; Labou, D.; Papakonstantinou, G.D.; Siokou, A.; Jaksic, M.M. Novel spillover interrelating reversible electrocatalysts for oxygen and hydrogen electrode reactions. *J. Phys. Chem. C* **2010**, *114*, 18298–18312. [CrossRef]
41. Lv, Q.; Yin, M.; Zhao, X.; Li, C.; Liu, C.; Xing, W. Promotion effect of TiO_2 on catalytic activity and stability of Pt catalyst for electrooxidation of methanol. *J. Power Sources* **2012**, *218*, 93–99. [CrossRef]
42. Gu, D.-M.; Chu, Y.-Y.; Wang, Z.-B.; Jiang, Z.-Z.; Yin, G.-P.; Liu, Y. Methanol oxidation on Pt/CeO_2–C electrocatalyst prepared by microwave-assisted ethylene glycol process. *Appl. Catal. B* **2011**, *102*, 9–18. [CrossRef]